UV Spectroscopy/Imaging and Science Questions

Paul Scowen (ASU)

Current Capabilities:

- GALEX: (Martin et al 2011)
  - 100 M$
  - Pegasus Launch
  - NASA Small Explorer
  - 0.5 meter telescope
  - 2 UV bands
  - Multiple Surveys
- HST/COS: (Green et al 2011)
  - 88 M$
  - Shuttle Installation (SM4)
  - NASA Great Observatory Instrument
  - 2.4m telescope
  - 2 UV channels

GALEX Optical System

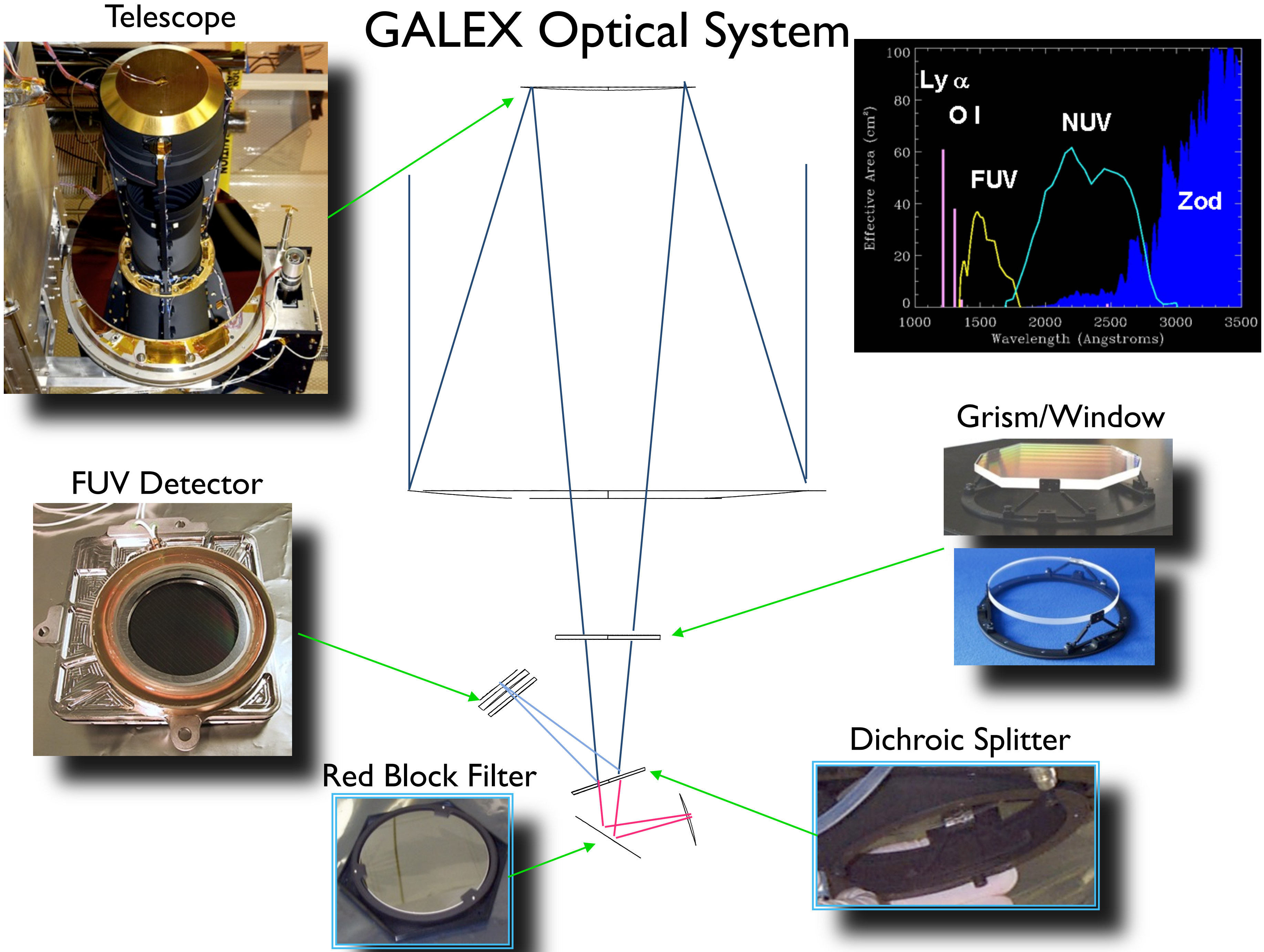

Design Highlights

TABLE 1

THE *GALEX* OPTICAL PRESCRIPTION

Parameter	Value
Telescope:	
Type	Ritchey-Chrétien
Coatings	MgF_2-coated Al
Primary diameter	500 mm
Secondary diameter	230 mm
Focal length	2998 mm
Focal ratio	6
Place scale	68.″80 mm^{-1}
Grism (CaF_2):	
Width (inscribed diameter)	124 mm
Thickness (center)	5.9 mm
Wedge	1.°37
Blaze angle	2.°33
Ruling	75 lines mm^{-1}
Imaging window (CaF_2):	
Diameter	124 mm
Thickness	6 mm
Dichroic (fused silica):	
Diameter	110 mm
Thickness	4 mm
Wedge	0.°119
Blue-edge filter (MgF_2):	
Diameter	74 mm
Thickness	2.5 mm
Red-blocking mirror:	
Diameter	110 mm

TABLE 2

SUMMARY OF MEASURED PERFORMANCE PARAMETERS FOR *GALEX*

Item	FUV Band	NUV Band
Bandwidth[a]	1344–1786 Å	1771–2831 Å
Effective wavelength[b]	1528 Å	2271 Å
Field of view	1.°28	1.°24
Peak effective area	36.8 cm^2 at 1480 Å	61.7 cm^2 at 2200 Å
Zero point (m_0)	18.82	20.08
Image resolution	4.″3 FWHM	5.″3 FWHM
Spectral resolution ($\lambda/\Delta\lambda$)	200	90
Detector background (typical):		
Total	78 counts s^{-1}	193 counts s^{-1}
Diffuse (cm^{-2})	0.66 counts s^{-1}	1.82 counts s^{-1}
Hot spots	47 counts s^{-1}	107 counts s^{-1}
Sky background (typical)[c]	2000 counts s^{-1}	20000 counts s^{-1}
Limiting magnitude (5 σ):[d]		
AIS (100 s)	19.9	20.8
MIS (1500 s)	22.6	22.7
DIS (30000 s)	24.8	24.4
Linearity:		
Global (10% rolloff)	18000 counts s^{-1}	
Global (50% rolloff)	91000 counts s^{-1}	
Local (10% rolloff)[e]	108 counts s^{-1}	295 counts s^{-1}
Pipeline image format	3840 × 3840 elements with 1.″5 pixels	

[a] The bandpass is defined by wavelengths with effective area at least 10% of the peak.

[b] From eq. (3) of Fukugita et al. (1996).

[c] These correspond to 690 and 745 photons s⁻ cm⁻ sr⁻Å ⁻, respectively.

[d] Approximate All-sky (AIS), Medium (MIS), and Deep (DIS) Imaging Survey depths.

[e] These are worst-case values for point sources.

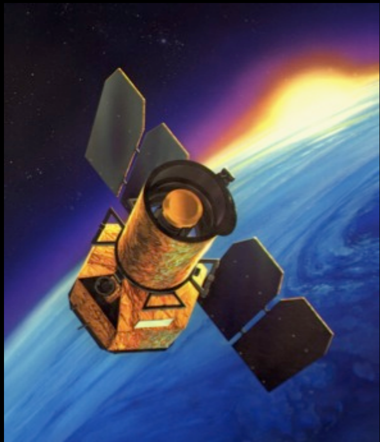

GALEX
Explorer
1250-2800Å

UV Sky Survey
All-Sky
Background
Maps

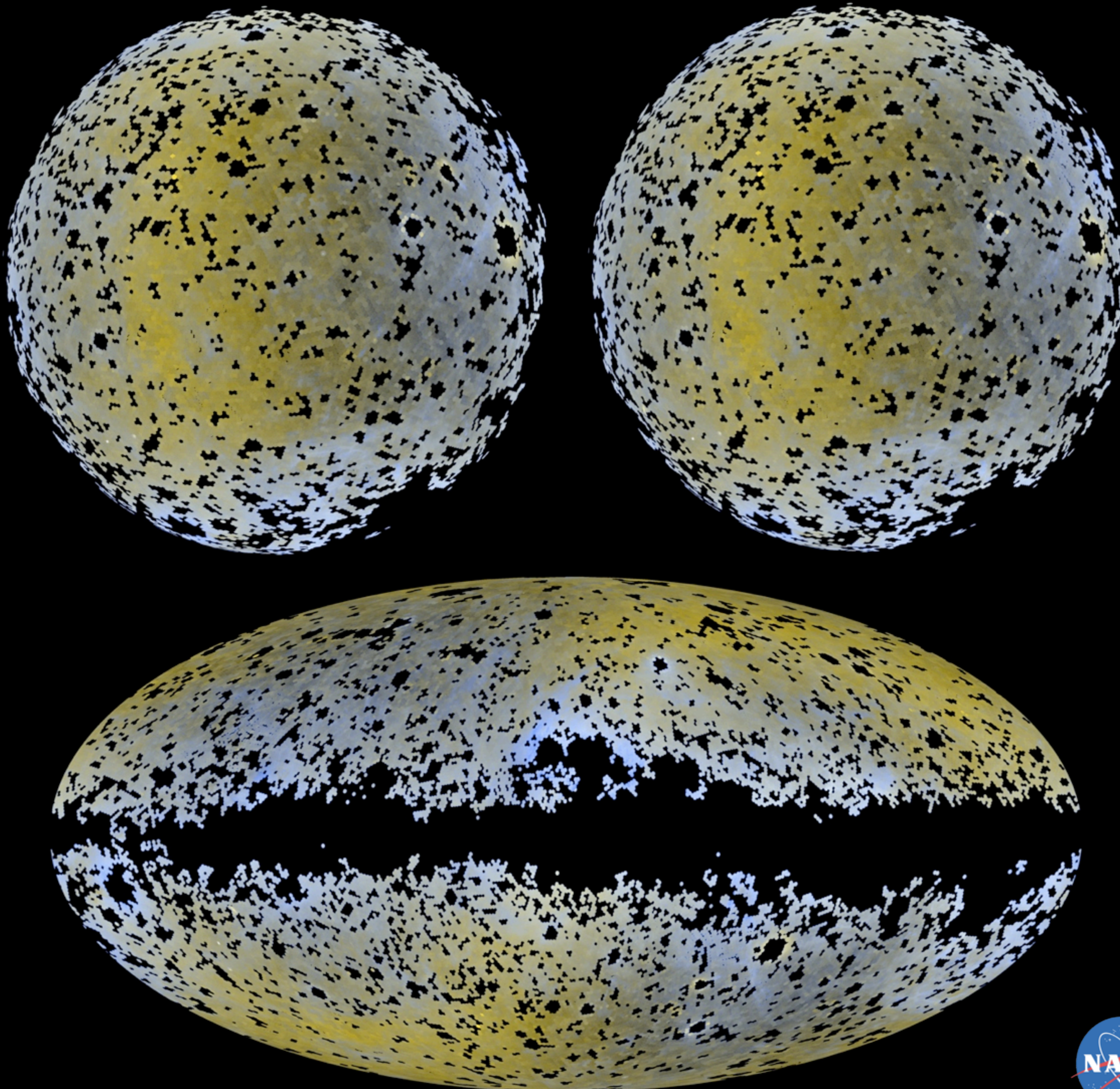

LMC Observations

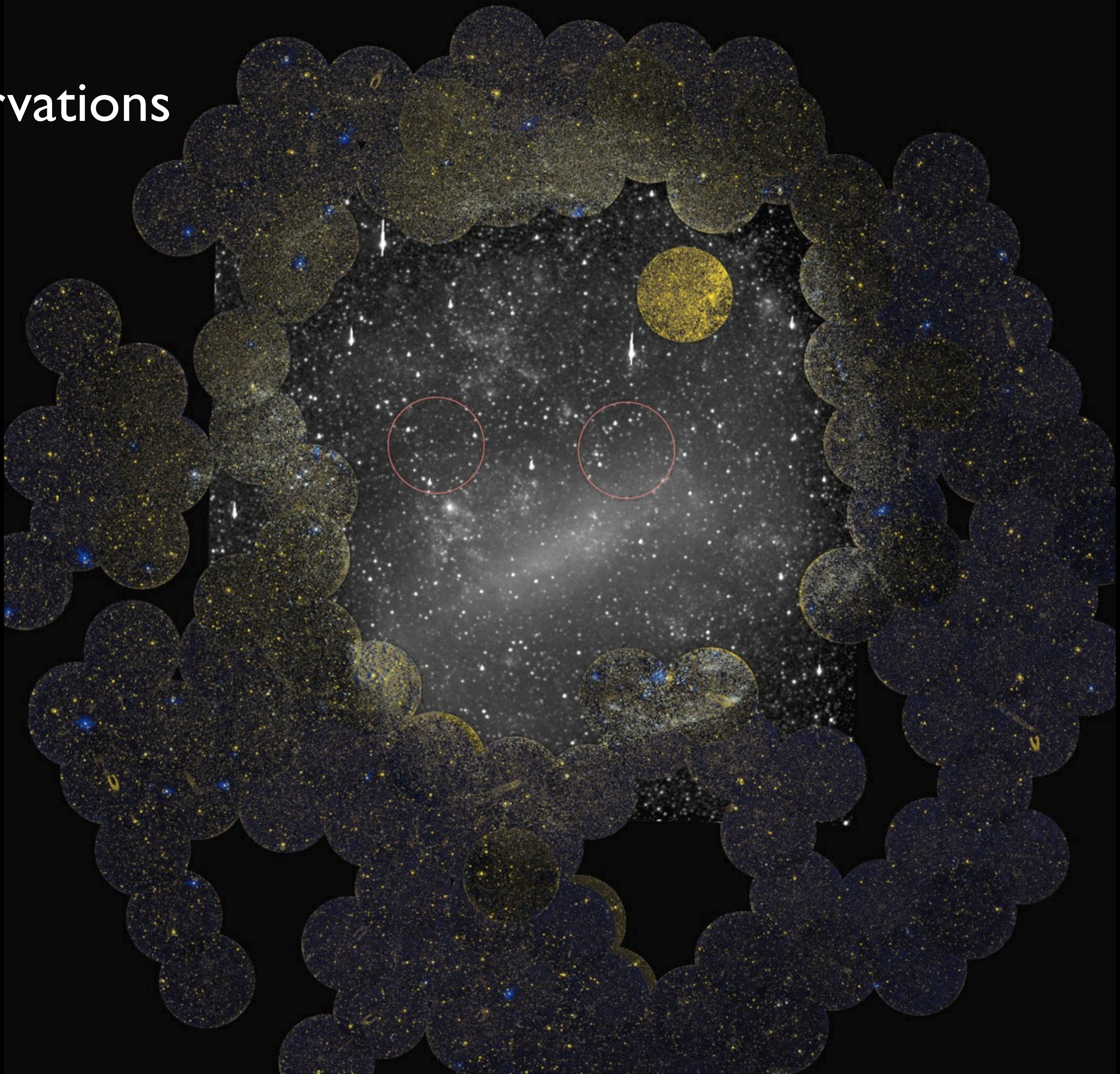

GALEX UV Traces Star Formation

Over Enormous Range of Specific Star Formation = SFR/MASS

Varying young + fixed old stellar pop

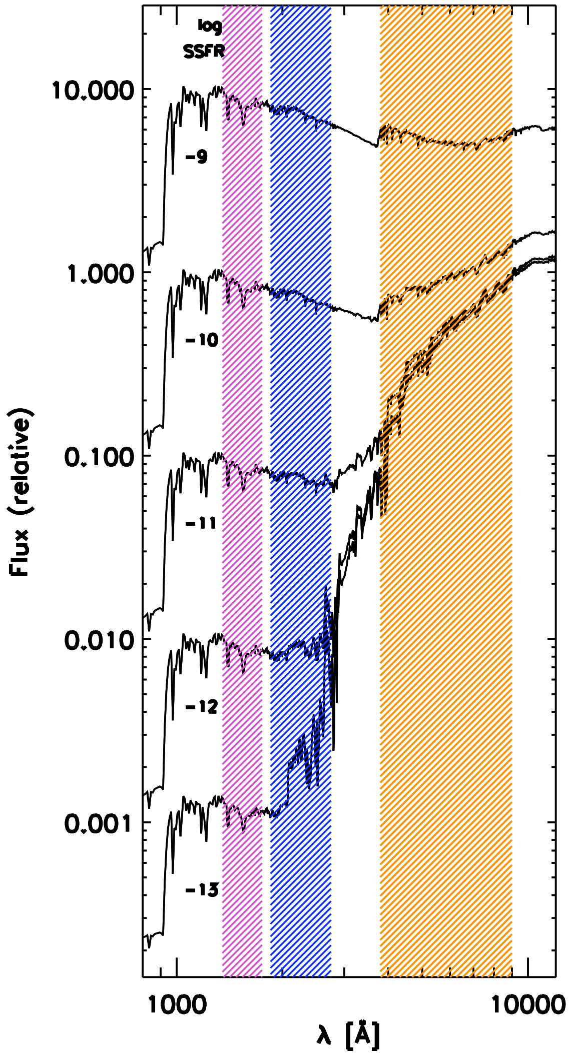

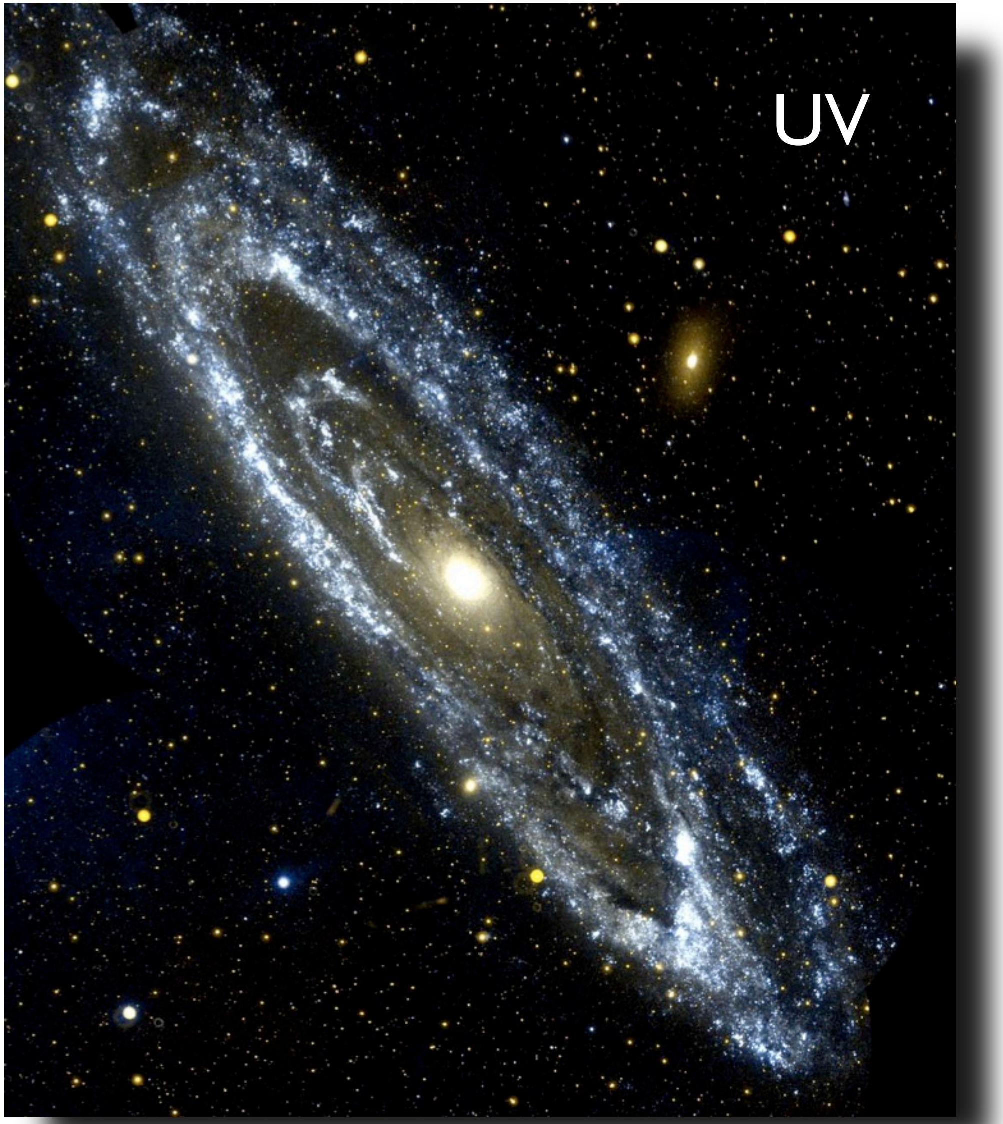

M31 optical: Adam Block/NOAO/AURA/NSF; UV: GALEX/JPL/NASA

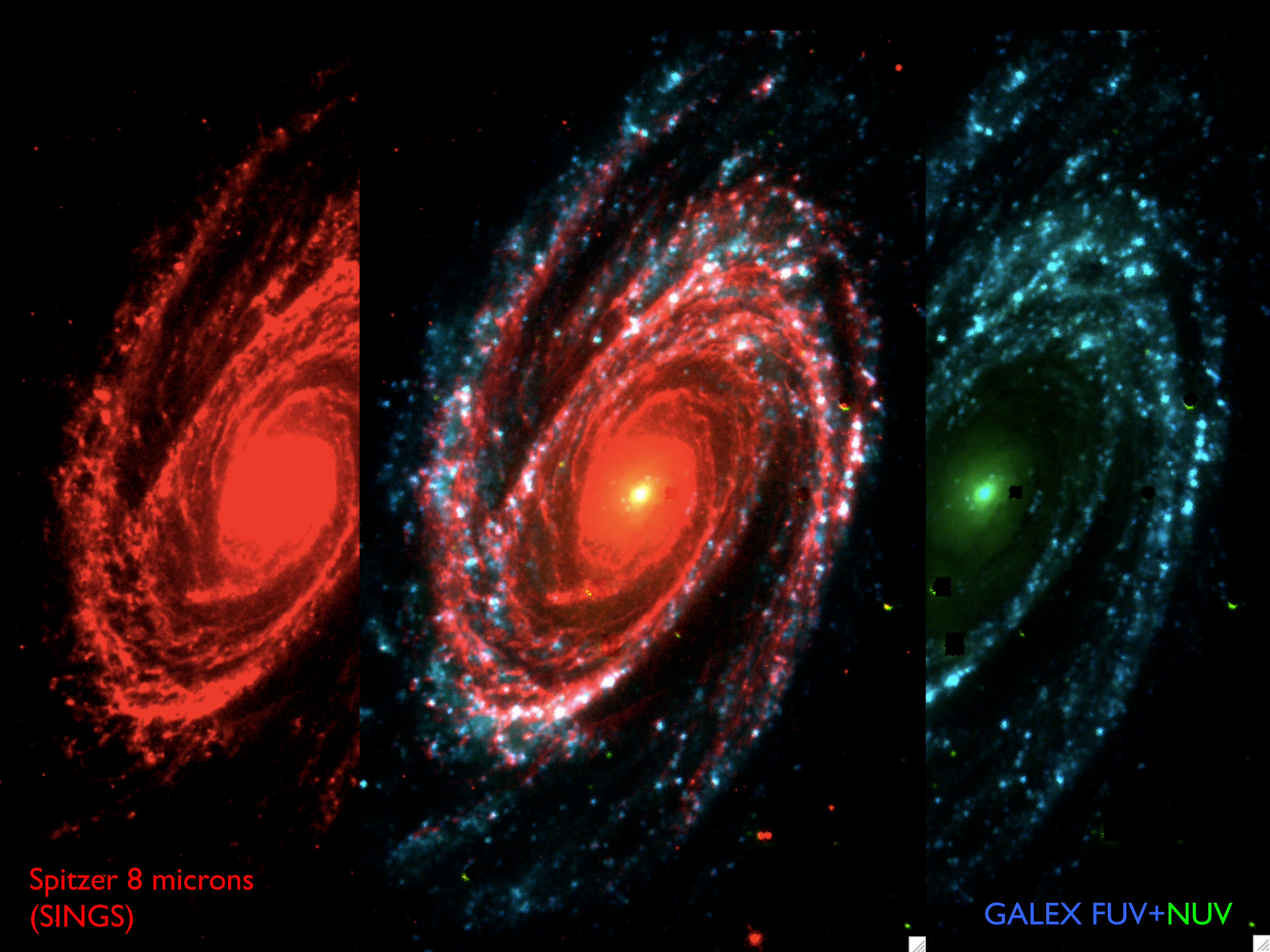
Spitzer 8 microns
(SINGS)
GALEX FUV+NUV

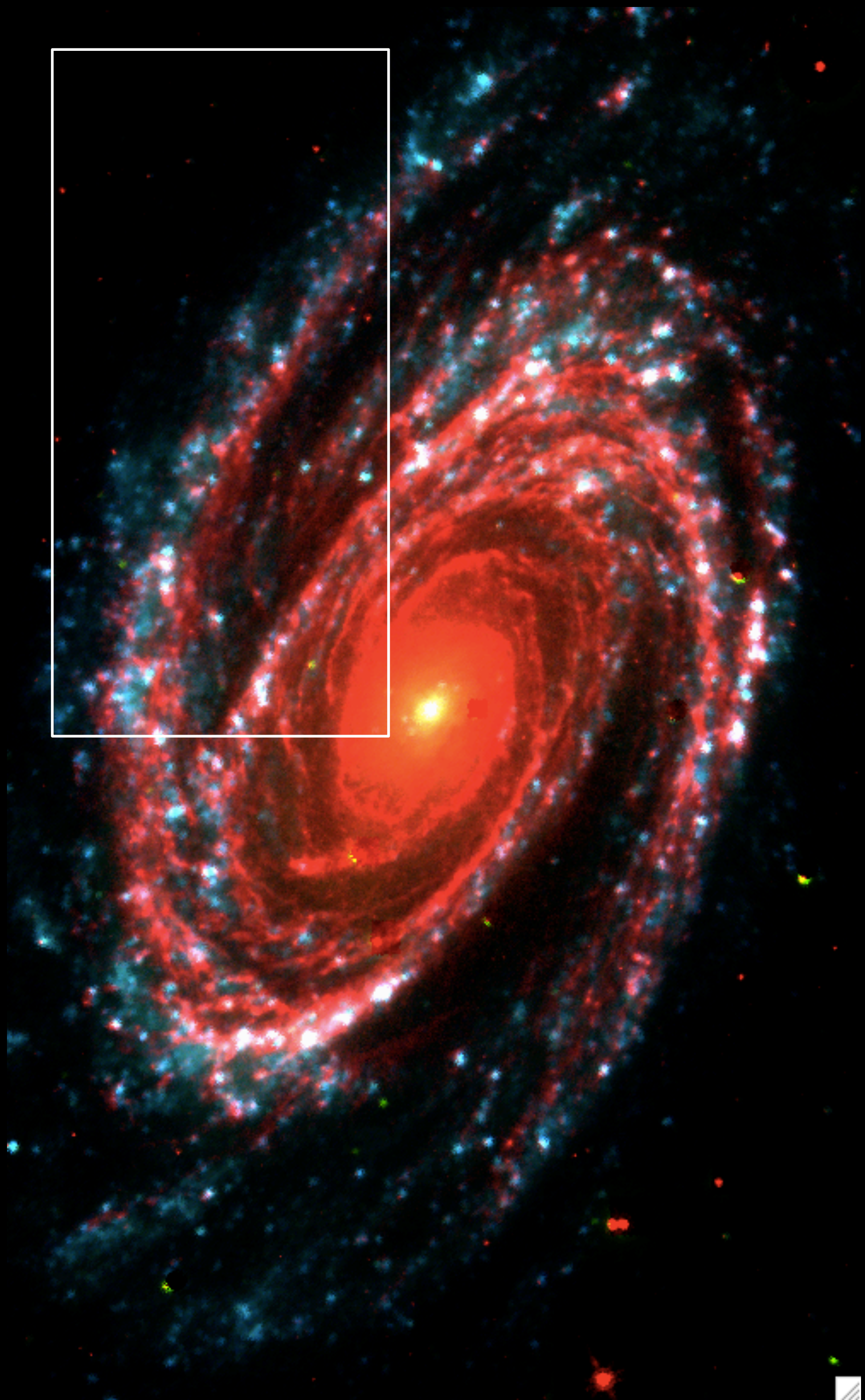

Spitzer 8 microns
(SINGS)

GALEX FUV+NUV

Stars vs. Dust

Star Formation History Delineated by Spiral Density Wave

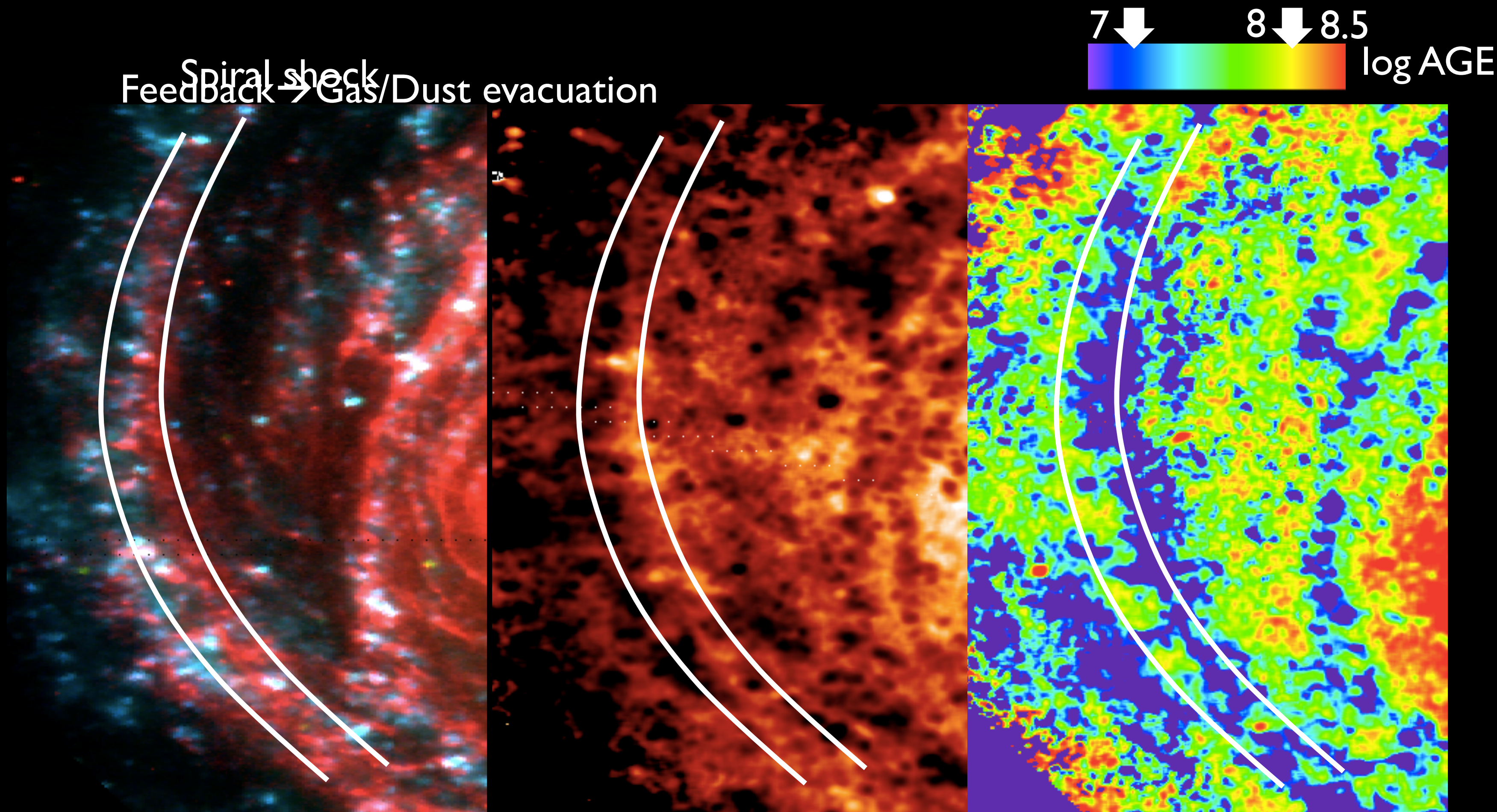

FIR NUV FUV → IRX = FIR/FUV

A_{FUV} + $[L_{FUV}/L_{NUV}](t)$ → AGE_{SSP}

Spitzer 8 μ m

GALEX NUV FUV

GALEX UV

in Local Analogs to High Redshift Galaxies

Lyman Break Galaxies z~3

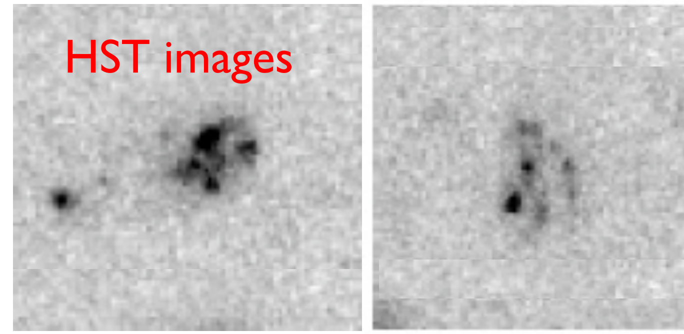

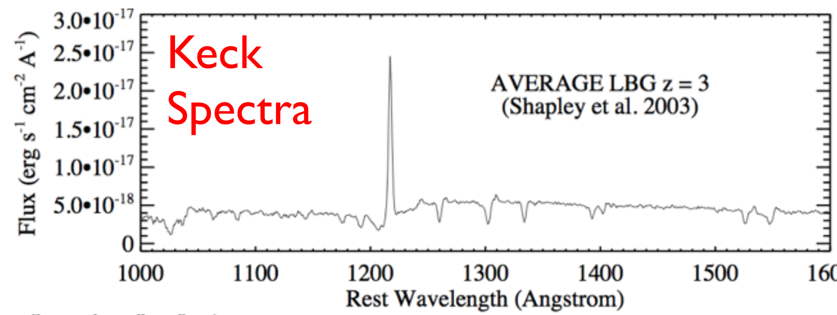

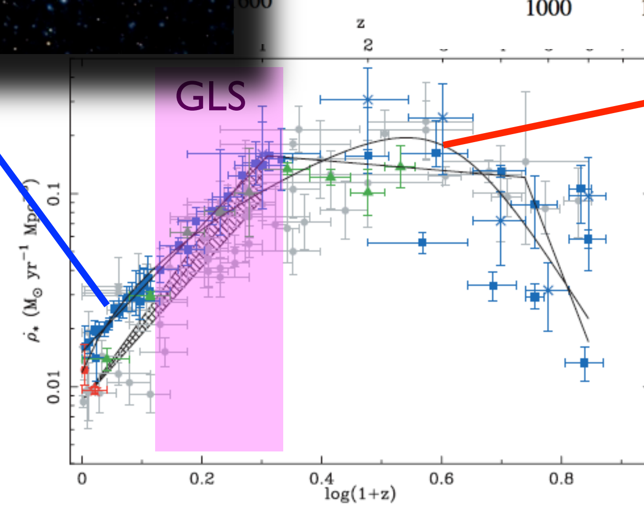

GALEX Legacy Survey discovers LBAs
z~0.2 → z~1.5
Missing link in galaxy evolution

H_2 Fluorescence in FUV
by-product of Photodissociation

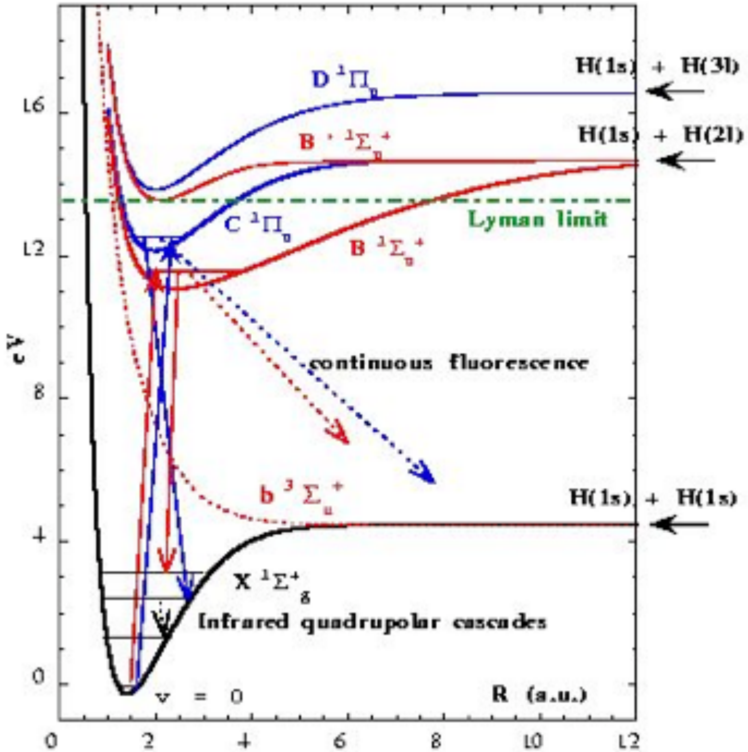

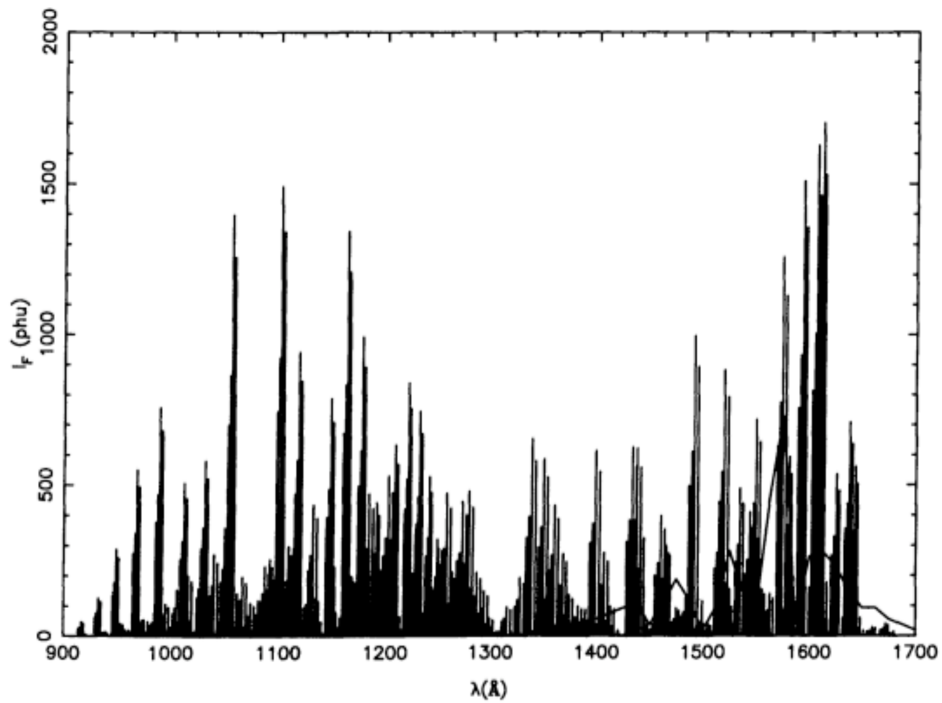

CW Leo – IRC 10216

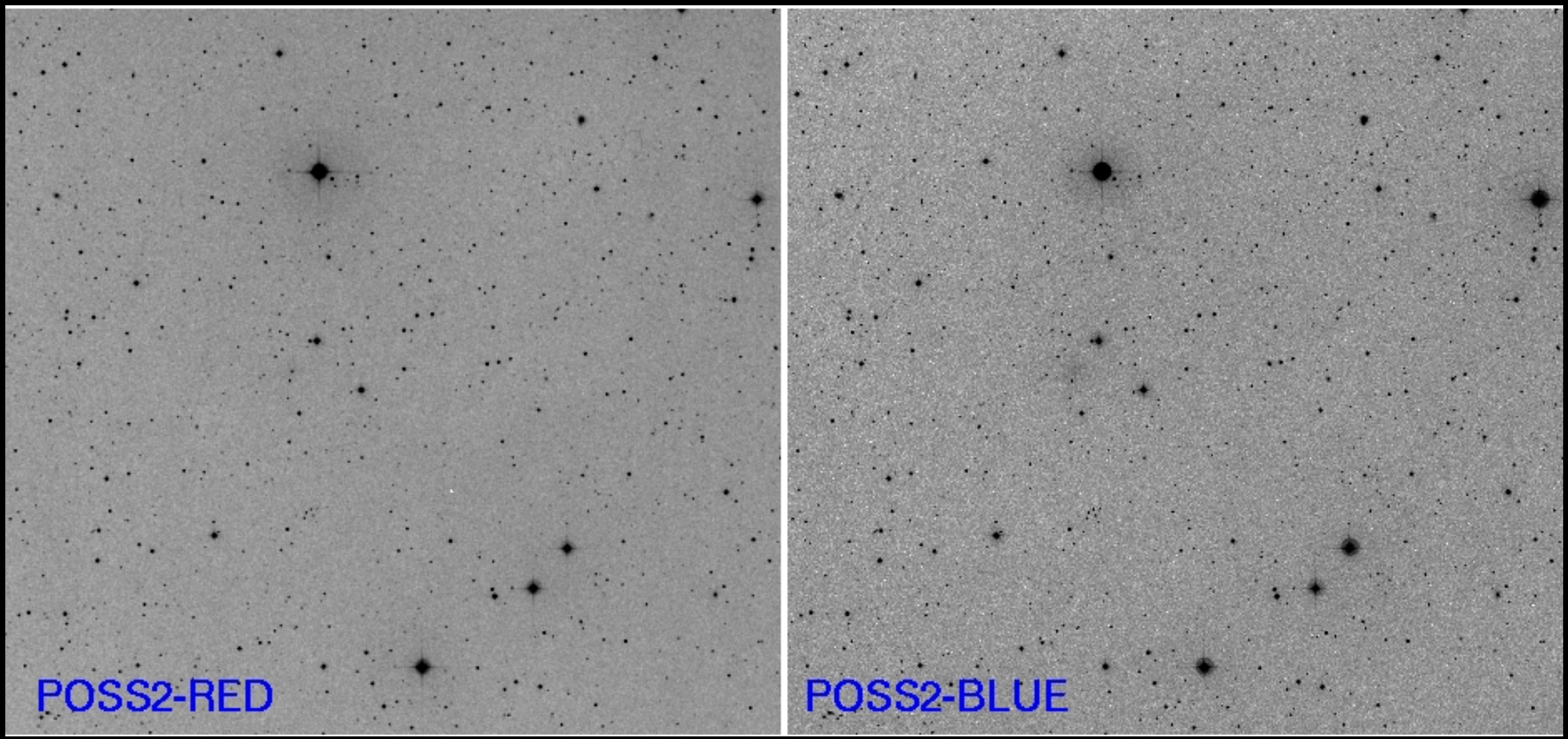

CW Leo – IRC 10216

H_2 Fluorescence & Dust Scattering

Dust Scattering

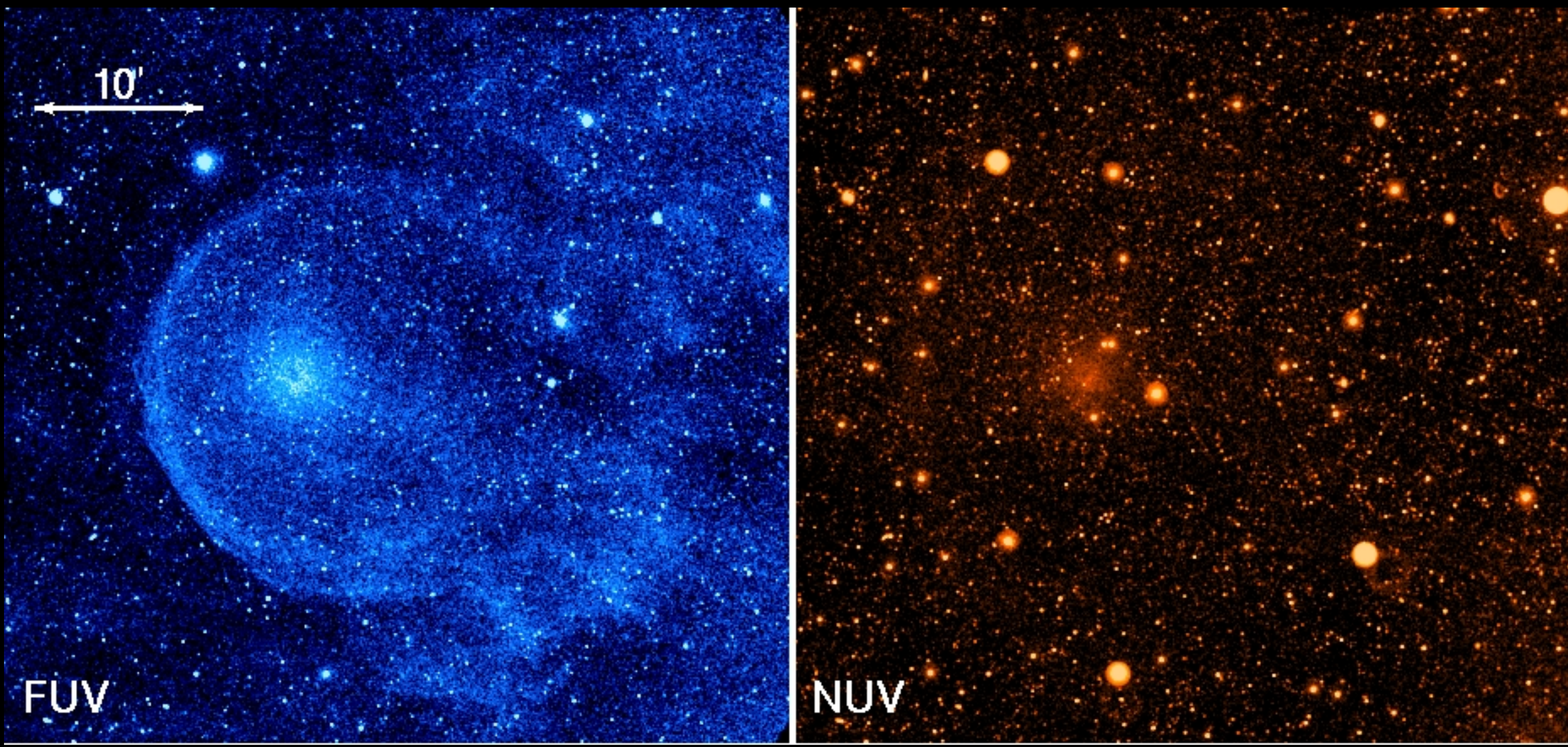

CW Leo: 1st "Astrosphere"

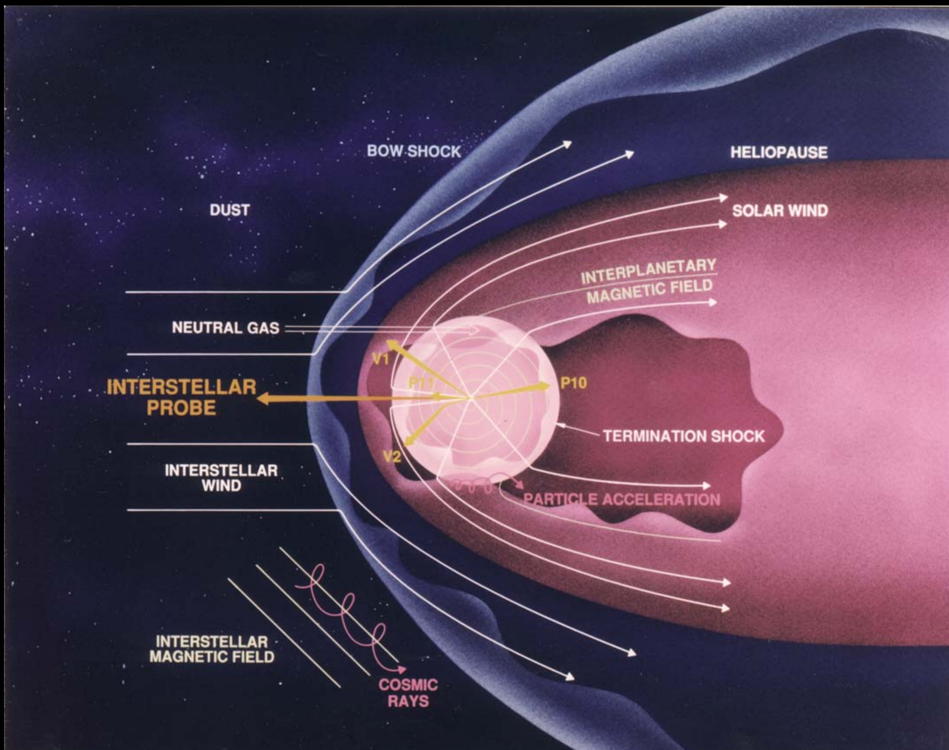

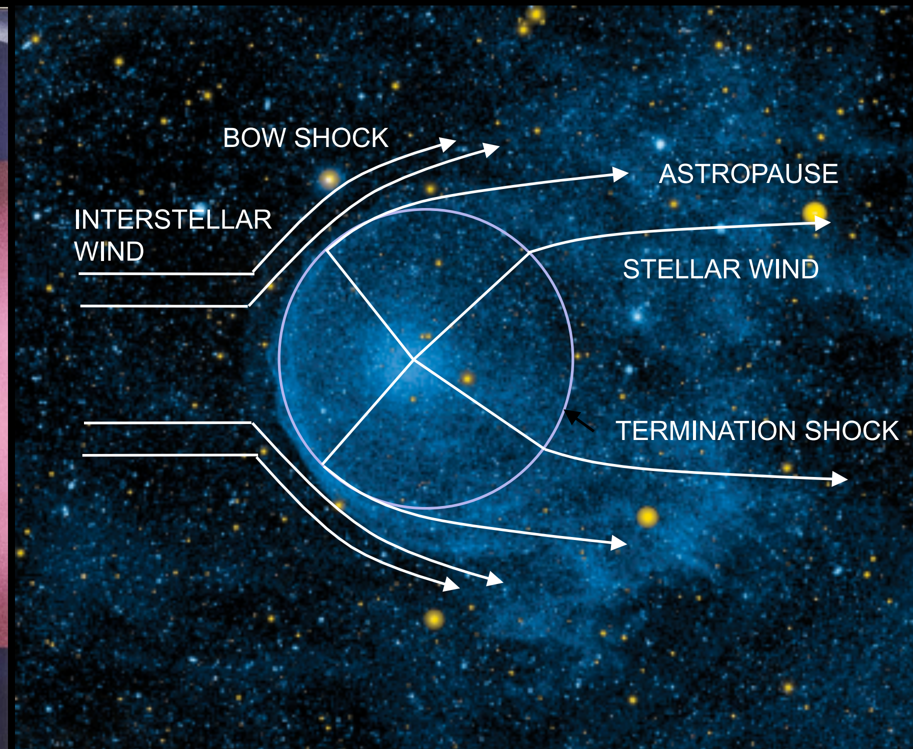

- CW Leo is first example of a complete "Astrosphere" analogous to Solar "Heliosphere"
- Inflowing ISM, Bow Shock, Astropause, Termination shock
- Physical scales are 10^4 x larger.

CW Leo: Asympotic Giant Branch Star

Evidence for Formation of Interstellar Clouds

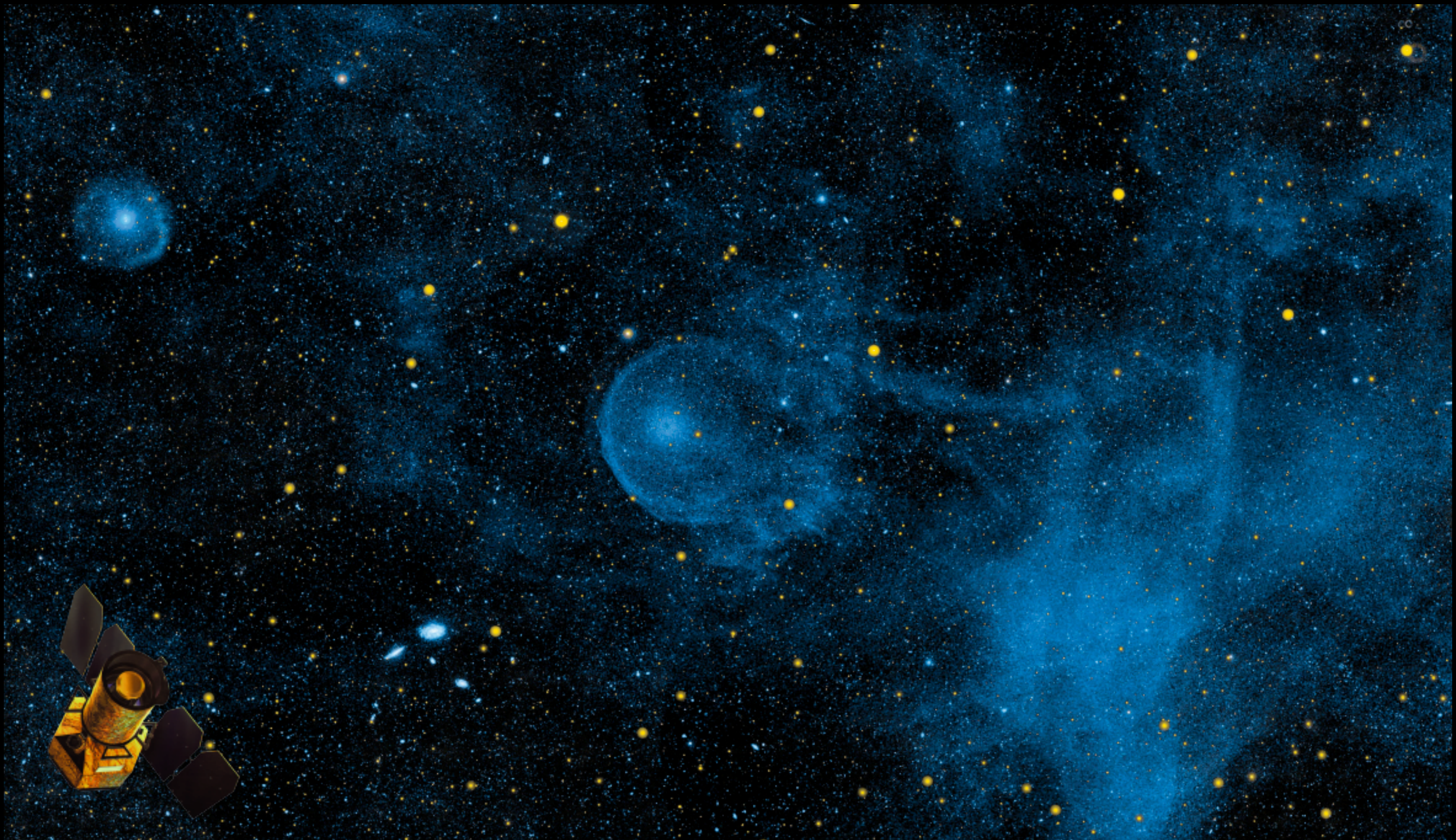

Seibert+2010

HST -COS

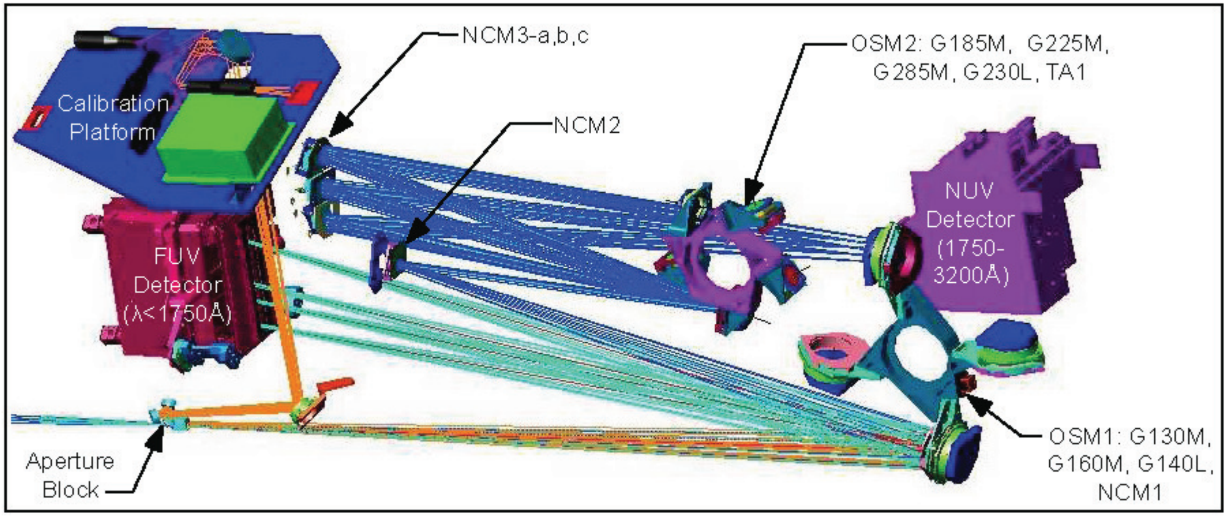

Fig. 1.— The COS optical layout showing the principal components of the instrument: OSM = Optical Select Mechanism, NCM = NUV Channel Mirror

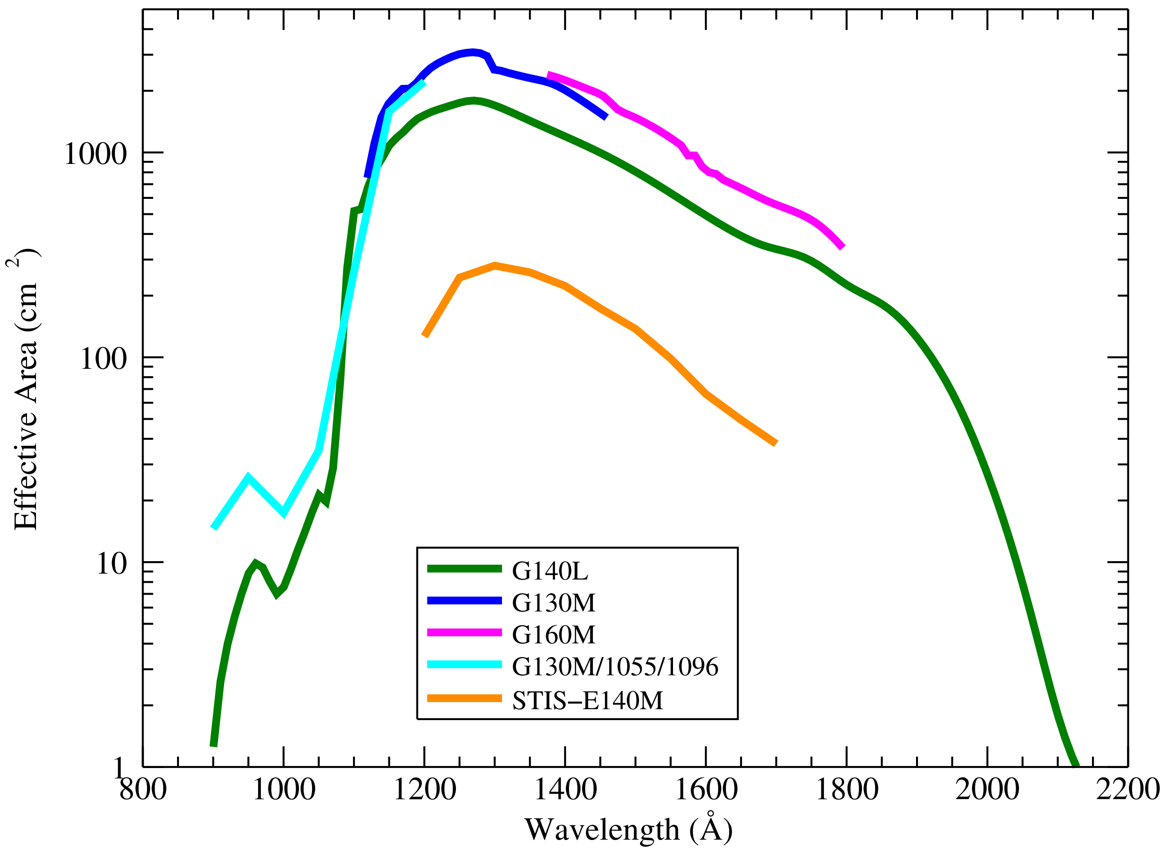

Fig. 4.— The measured, on-orbit effective area of the COS FUV channels. The nominal effective area for the STIS E140M channel is included for comparison. Slit transmission losses are not included for STIS.

Design Highlights

- Elimination of all transmissive optics
- Use of ion-etched holographic gratings to maximize efficiency
- Use of a large format detector (2 x 85mm x 10mm)
- Use of an opaque photocathode – higher DQE
- 2 channels: NUV – 175-320nm @ R=20,000; FUV – G130M and G160M, @ R=16,000-22,000
- Limiting Sensitivity ~ 1×10^{-17} ergs cm^{-2} sec^{-1} $Å^{-1}$

Observations of the IGM

- 90% of baryonic matter lies in the IGM
- Of that 30% is cool (10^4 K) and traced by Lyα forest and O VI line observations
- The warmer (10^5 K) 20-30% are traced by broad Lyα (BLA), O VI and Ne VIII absorption
- The hot phase comprises 40% at 10^6 K and are studied in X-rays via O VII and VIII
- In the UV, the warm and hot phases are accessed via absorption of Ne VIII, Mg X, Si XII and O VI as well as broad HI Lyα absorption

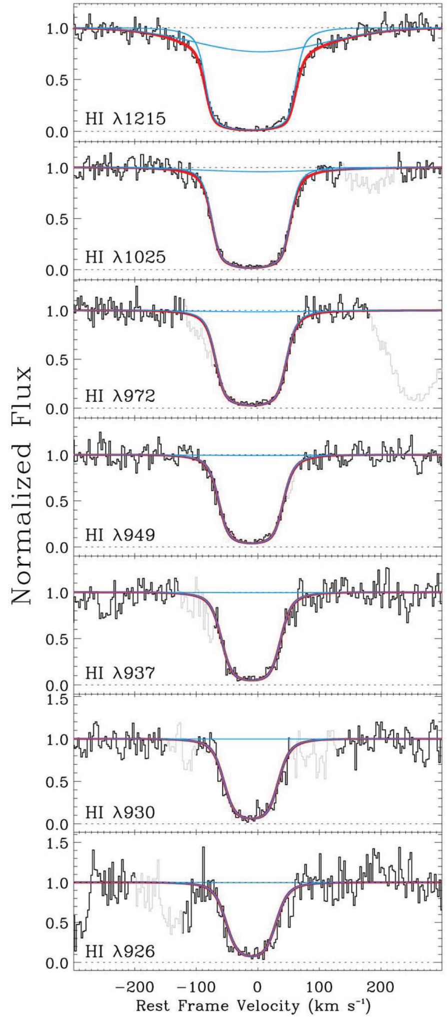

Fig. 11.— Simultaneous two-component Voigt profile fits to the COS observations of H I Lyman series (1216 to 926 Å) absorption at $z = 0.22601$ in the spectrum of the QSO HE 0153-4110 from Savage et al. (2011). The H I column density in the narrow H I component was determined to be log N(H I) $= 16.61^{+0.12}_{-0.17}$ from the Lyman Limit break in the FUSE observations of HE 0153-4520. The broad wings on Lyα require the presence of a BLA with log N(H I) $= 140^{+14}_{-16}$ km s^{-1} and log N (H I) $= 13.70^{+0.05}_{-0.08}$. The BLA is associated with the presence of strong O VI absorption in the multi-phase absorption system with log N(O VI) $= 14.21 \pm 0.02$ and b(O VI) $= 37 \pm 1$ km s^{-1} and implies the direct detection of hot gas in the IGM with log T $= 6.07^{+0.09}_{-0.12}$, [O/H] $= -0.28^{+0.09}_{-0.08}$ and log N(H) $= 20.41^{+0.13}_{-0.17}$.

Epochs of Reionization

- Probing the transition from neutral to ionized hydrogen in the IGM ($z \sim 7$-12)
- A corresponding helium transition occurred at $z \sim 2.8$, possibly fueled by quasars and AGN
- Absorption of the HeII Lyα line at 303.78nm has been seen around that redshift (Shull et al 2010)
- Troughs of strong absorption in the emission could correspond to filaments in the baryonic distribution
- Use of these HeII features provides access to measures of abundance variations as well as AGN source variations

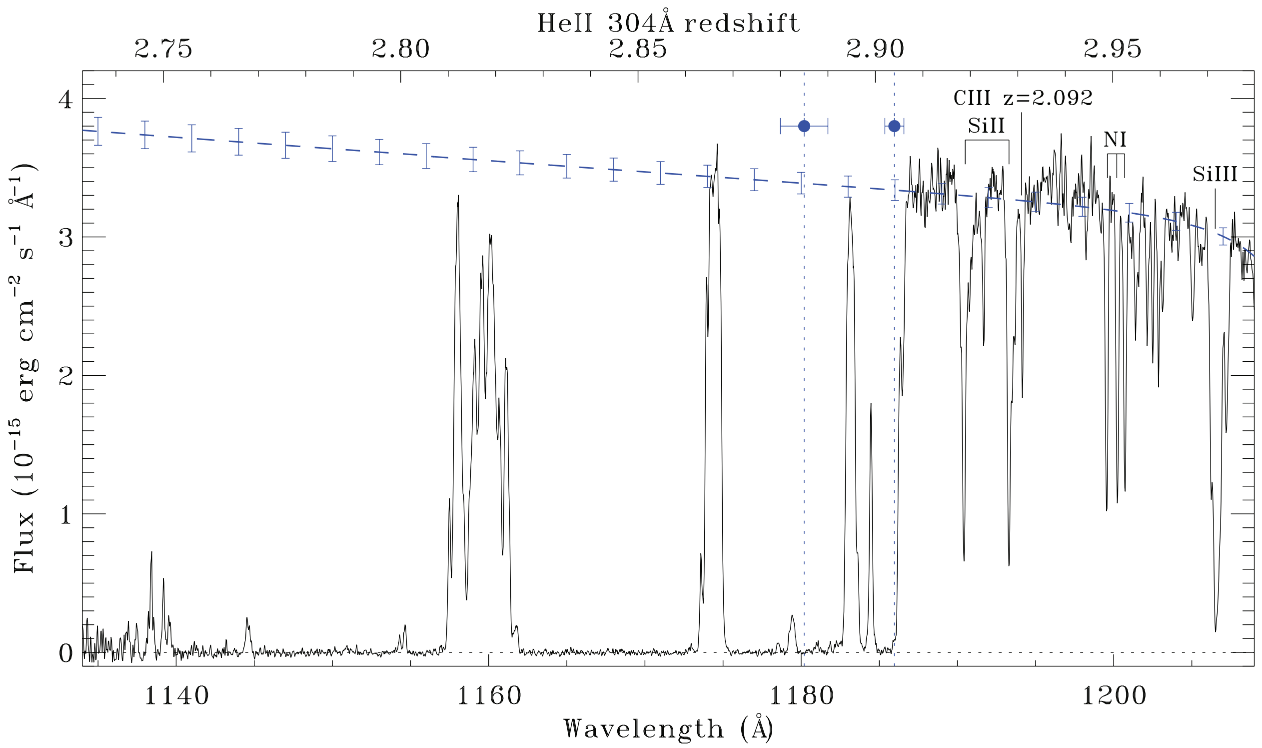

Fig. 12.— COS/G130M data (Shull et al. 2010) showing He II absorption troughs and flux transmission windows at redshifts $z \leq 2.9$. The proposed QSO systemic redshifts ($z_{\rm QSO} = 2.885$ and 2.904) and extrapolated AGN continuum are marked. Interstellar lines of N I, Si II, Si III appear longward of 1190 Å, and strong He II absorption is seen shortward of 1186.26 Å, with windows of flux transmission near 1183, 1174, 1160, and 1139 Å. Inexplicably, no QSO-proximity effect is seen in flux transmission near z = 2.86–2.90. Transmission recovers at $\lambda < 1100$ Å, shortward of three troughs of strong He II absorption ($\tau_{\rm HeII} \geq 5$) that span very large redshift intervals (and comoving radial distances) between z = 2.751–2.807 (61 Mpc), z = 2.823–2.860 (39 Mpc), and z = 2.868–2.892 (25 Mpc).

Star Forming Regions

- The use of Lyα emission to trace star formation rates – directly powered by ionization from young stars leading to H-recombination in the ISM
- The use is complicated by resonant scattering by atomic H leading to Lyα destruction by dust, and weaker lines, as well as ISM dynamics trapping Lyα photons
- Observational surveys of Lyα galaxies are needed to disentangle some of these effects, and at redshifts high enough to move beyond Galactic Lyα absorption
- The higher COS sensitivity has allowed a survey of 20 star forming galaxies that bracket ranges in abundance, dust and luminosity (Leitherer et al 2011, from Salzer et al 2000)

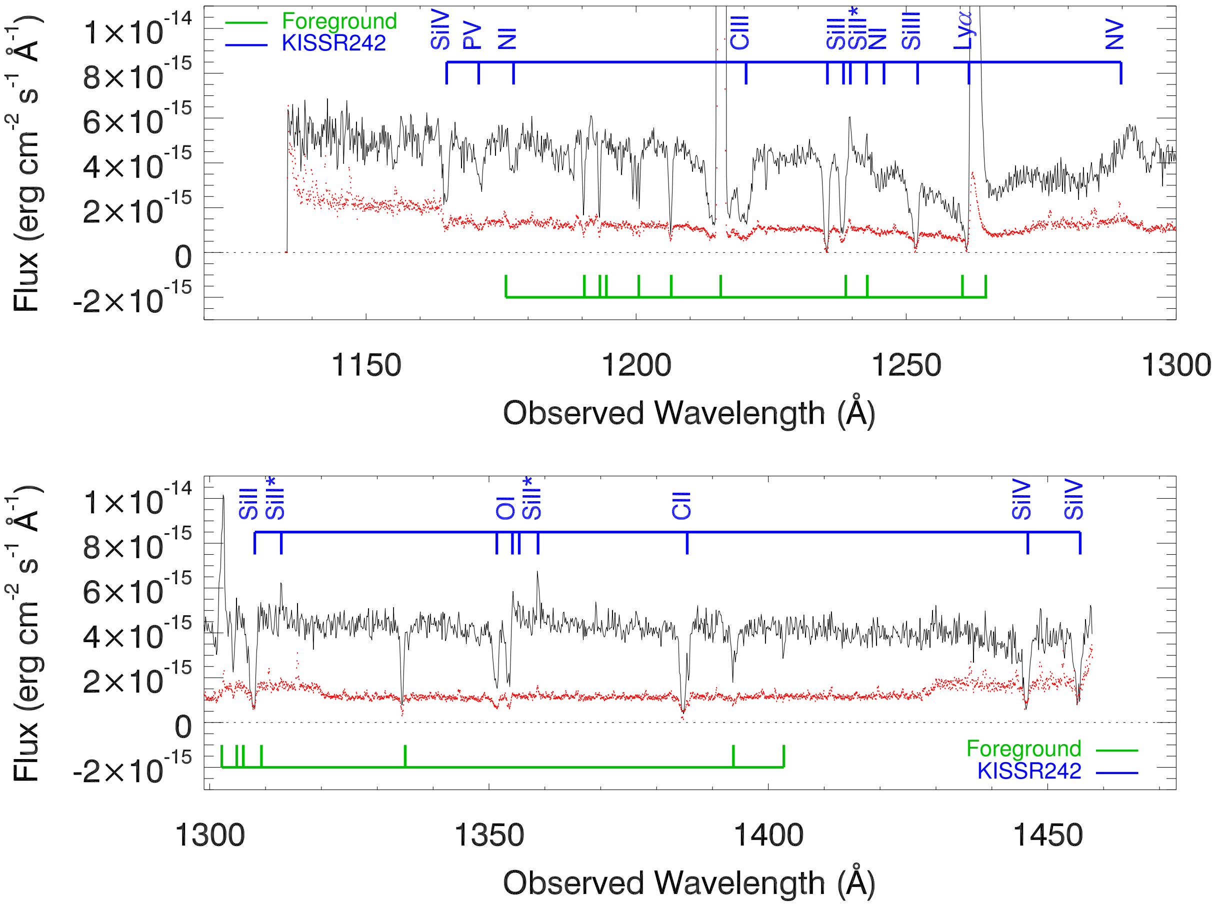

Fig. 15.— COS G130M rest-frame spectrum of the Hα selected galaxy KISSR0242, taken from the KISS database (Salzer et al. 2000). This spectrum (adapted from France et al. 2010b) was obtained in a single orbit using the G130M grating at two central wavelengths. The data are shown in black, with the error vector overplotted as the dotted red line. Foreground absorbers are identified with green tickmarks and the emission and absorption features at the redshift of KISSR0242 are labeled in blue.

Looking to the Future

- As part of a larger project, the UV offers both imaging and spectroscopic opportunities for a large aperture Observatory (4m)
- When combined with the optical and IR, the resulting wavelength baseline added to the larger field of view and better resolution and throughput can open doors to understand star and planet formation as a global process
- I offer here some highlights of design work from over the past 10 years (with thanks to Rolf Jansen, Sally Oey, Daniela Calzetti, Alex Fullerton, Jason Tumlinson, Patrick Hartigan, Steve Desch, Nathan Smith, Bob O'Connell and Ken Sembach among a host of others…)

Star Formation

- When combined with the optical and NIR, diffraction limited optics at 200-300nm will allow unprecedented precision in astrometry and photometry
- The ability to map billions of stars from the mid-UV to the near-IR to resolve stellar populations within and along the line of sight to Galactic SF regions – to become sensitive to variations in the IMF – and open multi-epoch measurements to look at time-variation in emission
- A comprehensive imaging survey of Galactic star-forming regions becomes possible, with the aim of tracking the evolution of circumstellar protoplanetary disks and other aspects of star formation in a wide variety of environments.
- This survey will combine multi-wavelength broad-band and key narrow-band imaging and will provide the measurements for color-color and color-magnitude diagram modeling of millions of young stars in a variety of evolutionary stages.
- This program will provide the basic data needed to understand star formation as a fundamental astrophysical process, will shed light on the apparent universality of the stellar IMF, and will be the cornerstone for interpreting measurements on star forming regions and global star formation properties in more distant galaxies.

Imaging Surveys of the Magellanic Clouds

- Assembly of a complete-area imaging survey of both Magellanic Clouds in 8 broad-band and 4 nebular emission-line filters that span the full 200–1100nm wavelength range
- This will allow:
  - Assembly of a complete census of the stellar populations within the Clouds
  - Investigation of the feedback from massive stars, both in H II-regions environments and in the diffuse, warm ISM
  - Quantitative parameterization of the stellar clustering properties
  - Determination of how giant, starbursting H II-regions like 30 Doradus differ from more modest H II-regions within the Milky Way
- A large aperture wide field of view UV/optical camera could map both Magellanic Clouds in their entirety at <0.″1–0′.′15 spatial resolution in 8 broad-band filters spanning the mid-UV (~225 nm) through near-IR (Y ; λ_c = 1020 nm) to m_{AB} >26 mag and in 4 key narrow-band filters to ~10^{-16} erg cm^{-2} s^{-1} arcsec^{-2}
- It would be possible to also image 21 H II-regions through 3 additional narrow- band filters, to provide more detailed nebular diagnostics that are used to understand these star-formation environments in terms of what we learned at even smaller scales in our own Galaxy.

Survey of Nearby Galaxy Populations

- To learn how galaxies work through studies of their stars, ISM, and immediate environments. This program consists of two complementary parts.

- The first part provides deep observations of a moderate- sized sample of ~ 100 nearby galaxies using a set of broad- and narrow-band filters that span the 200–1100 nm wavelength range. We will be able to analyze the resolved and unresolved stellar populations in 100 archetypical galaxies through color-magnitude and color-color diagram fitting and population synthesis modeling of multi-band colors and will yield physical properties such as spatially resolved star formation histories.

- The ISM in each galaxy can be analyzed using key narrow-band filters that distinguish photospheric from shock heating and provide information on the metallicity of the gas

- The second part provides medium-deep observations of a larger number (~ 500) galaxies through a subset of these filters. We will be able to sample, and provide statistics for, the full parameter space of physical conditions and environments in which stars form and will place the deeper, detailed properties of *the* first survey in the broader context of the galaxy environments — their satellite systems and interface with the cosmic web.

- These programs require a large (~ 14′×14′) field of view, wavelength agility, sensitivity, and angular resolution. They would represent the first *comprehensive* galaxy surveys at 0.″04 –0.″13 (200–1100nm) diffraction-limited resolution, providing a 21st century digital standard for testing our understanding of the processes that affect the assembly and evolution of galaxies of different forms and mass.

YSOs, Protoplanetary Disks and Extrasolar Giant Planets

- Using FUV spectroscopy behind a 4m-class aperture we can measure accretion rates in intermediate mass young stars from the strong UV lines emitted as material strikes the stellar surface

- There is some hope we could observe FUV absorption spectra and fluorescent emission to measure H_2 and directly measure the disk gas mass around a protoplanetary disk – this will provide a more sensitive measure than we can achieve in NIR or MIR spectroscopy

- Transit spectroscopy of hot Jupiters in the FUV where atomic species have strong absorption lines will allow us to determine atmospheric components, interior structure, and evaporation rates

Diagnostics of Bipolar Outflows

- Using NUV lines such as MgII we can high spatial and velocity resolution measurements of outflow dynamics
- This can diagnose the launch mechanism and tie it to the nature of the accretion from the disk and how that material ultimately makes it onto the stellar body, as well as rotation rates
- To solve these kinds of problems we need resolutions of 10's of AU in Taurus (0.07") and spectral resolution above 10,000 with a low UV background

Mapping of Planetary and Asteroidal Surfaces

- The UV is a key bandpass for measuring different mineral properties – many become strongly absorbing in the UV allowing detection and mapping of particular mineral classes
- On the Moon these techniques can be used to constrain the abundance and distribution of TiO_2
- On Minor Bodies we can use the UV to better define the taxonomic classes of asteroids based on their body materials as well as aqueous alteration and thermal metamorphism, as well as detecting metals

Star Formation in Metal-Poor Environments

- Execute a survey of hundreds of sight lines into the Magellanic Clouds toward OB stars
- Can use a large number of key diagnostics in the UV: H_2, Ar I, O VI, Fe II, Lyβ and Lyα, N V, and [O I]
- Quantitative analysis of temperatures, densities, compositions, and kinematics of the gas, as well as the properties of the OB-stars themselves
- These nearest extragalactic systems offer access to star-forming regions differing up to a factor 5 in metallicity, and the nearest example of a starburst environment.

Origin of Galaxies

- Modern galaxies accrete their material from the intergalactic medium (IGM)
- They also return metals, and energy, through supernova driven outflows, merger debris and tidal interactions
- The signature of these processes is imprinted on the interface zone between galaxies and the IGM
- Far-UV spectroscopic observations would allow us to simultaneously measure the “hot” and “cold” baryon populations, the return rate and feedback mechanisms, and look for the missing baryons.